

Effects of Landau-Lifshitz-Gilbert damping on domain growth

Kazue Kudo

*Department of Computer Science, Ochanomizu University,
2-1-1 Ohtsuka, Bunkyo-ku, Tokyo 112-8610, Japan*

(Dated: December 3, 2024)

Domain patterns are simulated by the Landau-Lifshitz-Gilbert (LLG) equation with an easy-axis anisotropy. If the Gilbert damping is removed from the LLG equation, it merely describes the precession of magnetization with a ferromagnetic interaction. However, even without the damping, domains that look similar to those of scalar fields are formed, and they grow with time. It is demonstrated that the damping has no significant effects on domain growth laws and large-scale domain structure. In contrast, small-scale domain structure is affected by the damping. The difference in small-scale structure arises from energy dissipation due to the damping.

PACS numbers: 89.75.Kd, 89.75.Da, 75.10.Hk

I. INTRODUCTION

Coarsening or phase-ordering dynamics is observed in a wide variety of systems. When a system is quenched from a disordered phase to an ordered phase, many small domains are formed, and they grow with time. For example, in the case of an Ising ferromagnet, up-spin and down-spin domains are formed, and the characteristic length scale increases with time. The Ising spins can be interpreted as two different kinds of atoms in the case of a binary alloy. At the late stage of domain growth in these systems, characteristic length $L(t)$ follows a power-law growth law,

$$L(t) \sim t^n, \quad (1)$$

where n is the growth exponent. The growth laws in scalar fields have been derived by several groups: $n = 1/2$ for non-conserved scalar fields, and $n = 1/3$ for conserved scalar fields [1–8].

Similar coarsening dynamics and domain growth have been observed also in Bose-Einstein condensates (BECs). The characteristic length grows as $L(t) \sim t^{2/3}$ in two-dimensional (2D) binary BECs and ferromagnetic BECs with an easy-axis anisotropy [9–11]. The same growth exponent $n = 2/3$ is found in classical binary fluids in the inertial hydrodynamic regime [1, 12]. It is remarkable that the same growth law is found in both quantum and classical systems. It should be also noted that domain formation and coarsening in BECs occur even without energy dissipation. The dynamics in a ferromagnetic BEC can be described approximately by an extended Landau-Lifshitz-Gilbert (LLG) equation in which the interaction between superfluid flow and local magnetization is incorporated [9, 13]. The normal LLG equation is usually used to describe spin dynamics in a ferromagnet. The LLG equation includes a damping term which is called the Gilbert damping. When the system has an easy-axis anisotropy, the damping has the effect to direct a spin to the easy-axis direction. The Gilbert damping in the LLG equation corresponds to energy dissipation in a BEC. In other words, domain formation without energy dissipation in a BEC implies that domains can be

formed without the damping in a ferromagnet. However, the LLG equation without the damping describes merely the precession of magnetization with a ferromagnetic interaction.

In this paper, we focus on what effects the damping has on domain formation and domain growth. Using the LLG equation (without flow terms), we investigate the magnetic domain growth in a 2D system with an easy-axis anisotropy. Since our system is simpler than a BEC, we can also give simpler discussions on what causes domain formation in the case where no energy dissipation or damping exists. When the easy axis is perpendicular to the x - y plain, the system is an Ising-like ferromagnetic film, and domains in which the z component of each spin has almost the same value are formed. Without the damping, the z component is conserved. The damping breaks the conservation of the z component as well as energy. Here, we should note that the growth laws for conserved and nonconserved scalar fields cannot simply be applied to the no-damping and damping cases, respectively, in our system. Although the z component corresponds to the order parameter of a scalar field, our system has the other two components. It is uncertain whether the difference in the number of degrees of freedom can be neglected in domain formation.

The rest of the paper is organized as follows. In Sec. II, we describe the model and numerical procedures. Energies and the characteristic length scale are also introduced in this section. Results of numerical simulations are shown in Sec. III. Domain patterns at different times and the time evolution of energies and the average domain size are demonstrated. Scaling behavior is confirmed in correlation functions and structure factors at late times. In Sec. IV, we discuss why domain formation can occur even in the no-damping case. Finally, conclusions are given in Sec. V.

II. MODEL AND METHOD

The model we use in numerical simulations is the LLG equation, which is widely used to describe the spin dy-

namics in ferromagnets. The dimensionless normalized form of the LLG equation is written as

$$\frac{\partial \mathbf{m}}{\partial t} = -\mathbf{m} \times \mathbf{h}_{\text{eff}} + \alpha \mathbf{m} \times \frac{\partial \mathbf{m}}{\partial t}, \quad (2)$$

where \mathbf{m} is the unit vector of spin, α is the dimensionless Gilbert damping parameter. We here consider the 2D system lying in the x - y plane, and assume that the system has a uniaxial anisotropy in the z direction and that no long-range interaction exists. Then, the dimensionless effective field is given by

$$\mathbf{h}_{\text{eff}} = \nabla^2 \mathbf{m} + C_{\text{ani}} m_z \hat{\mathbf{z}}, \quad (3)$$

where C_{ani} is the anisotropy parameter, and $\hat{\mathbf{z}}$ is the unit vector in the z direction.

Equation (2) is mathematically equivalent to

$$\frac{\partial \mathbf{m}}{\partial t} = -\frac{1}{1 + \alpha^2} \mathbf{m} \times \mathbf{h}_{\text{eff}} + \frac{\alpha}{1 + \alpha^2} \mathbf{m} \times (\mathbf{m} \times \mathbf{h}_{\text{eff}}). \quad (4)$$

Solving Eq. (4), we perform numerical simulations. The initial condition is given as spins that are aligned in the x direction with a little random noises: $m_x \simeq 1$ and $m_y \simeq m_z \simeq 0$. Simulations are performed in the 512×512 lattice with periodic boundary conditions. Averages are taken over 20 independent runs.

The energy in this system is written as

$$\begin{aligned} E &= E_{\text{int}} + E_{\text{ani}} \\ &= \int d\mathbf{r} (\nabla \mathbf{m}(\mathbf{r}))^2 - C_{\text{ani}} \int d\mathbf{r} m_z(\mathbf{r})^2, \end{aligned} \quad (5)$$

which gives the effective field as $\mathbf{h}_{\text{eff}} = -\delta E / \delta \mathbf{m}$. The first and second terms are the interfacial and anisotropy energies, respectively. When $C_{\text{ani}} > 0$, the z component becomes dominant since a large m_z^2 lowers the energy. We take $C_{\text{ani}} = 0.2$ in the simulations. The damping parameter α expresses the rate of energy dissipation. If $\alpha = 0$, the spatial average of m_z as well as the energy E is conserved.

Considering m_z as the order parameter of this system, we here define the characteristic length scale L of a domain pattern from the correlation function

$$G(\mathbf{r}) = \frac{1}{A} \int d^2 \mathbf{x} \langle m_z(\mathbf{x} + \mathbf{r}) m_z(\mathbf{x}) \rangle, \quad (6)$$

where A is the area of the system and $\langle \cdots \rangle$ denotes an ensemble average. The average domain size L is defined by the distance where $G(r)$, i.e., the azimuth average of $G(\mathbf{r})$, first drops to zero, and thus, $G(L) = 0$.

III. SIMULATIONS

Domain patterns appear, regardless of the damping parameter α . The snapshots of the no-damping ($\alpha = 0$) and

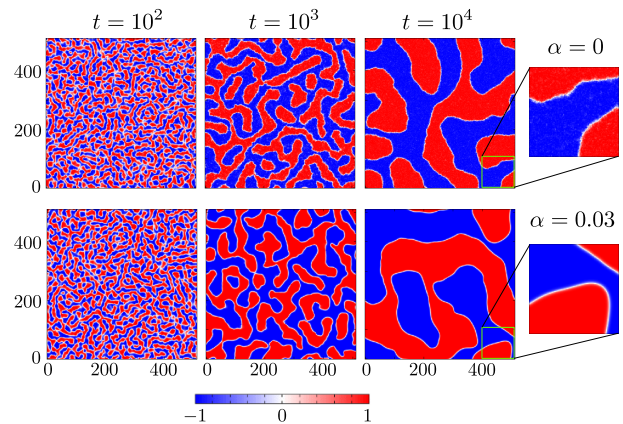


FIG. 1. (Color online) Snapshots of z -component m_z at time $t = 10^2$, 10^3 , and 10^4 . Upper and lower rows are for the no-damping ($\alpha = 0$) and damping ($\alpha = 0.03$) cases, respectively. Rightmost snapshots are enlarged ones at $t = 10^4$.

damping ($\alpha = 0.03$) cases are demonstrated in the upper and lower rows of Fig. 1, respectively. Domain patterns at early times have no remarkable difference between the two cases. At later times, as shown in the enlarged snapshots, difference appears especially around domain walls, although the characteristic length scale looks almost the same. Domain walls, where $m_z \simeq 0$, are smooth in the damping case. However, in the no-damping case, they look fuzzy, and small fractions of white ($m_z = 0$) area are embedded in red ($m_z = 1$) and blue ($m_z = -1$) areas.

The difference in domain structure is closely connected with energy dissipation, which is shown in Fig. 2. The interfacial energy, which is the first term of Eq. (5), decays for $\alpha = 0.03$ but increases for $\alpha = 0$ in Fig. 2 (a). In contrast, the anisotropy energy, which comes from the total of m_z^2 , decreases with time for both $\alpha = 0$ and $\alpha = 0.03$. In other words, the energy dissipation relating to the interfacial energy mainly causes the difference between the damping and no-damping cases. In the damping case, the interfacial energy decreases with time after a short-time increase as domain-wall structure becomes smooth. However, in the no-damping case, the interfacial energy increases with time to conserve the energy that is given by Eq. (5). This implies that the domain structure does not become smooth in the no-damping case.

In Fig. 3, the average domain size L is plotted for the damping and no-damping cases. The growth exponents of both cases change from about $n = 1/3$ to $n = 1/2$. The change in growth exponent is related with the saturation of m_z . How m_z saturates is reflected in the time dependence of the anisotropy energy which is shown in Fig. 2(b). At early times ($t \lesssim 1000$), when the average domain size grows as $L(t) \sim t^{1/3}$, E_{ani} decays rapidly. This implies that m_z is not saturated enough in this time regime. The decrease in the anisotropy energy slows at late times, then the average domain size grows

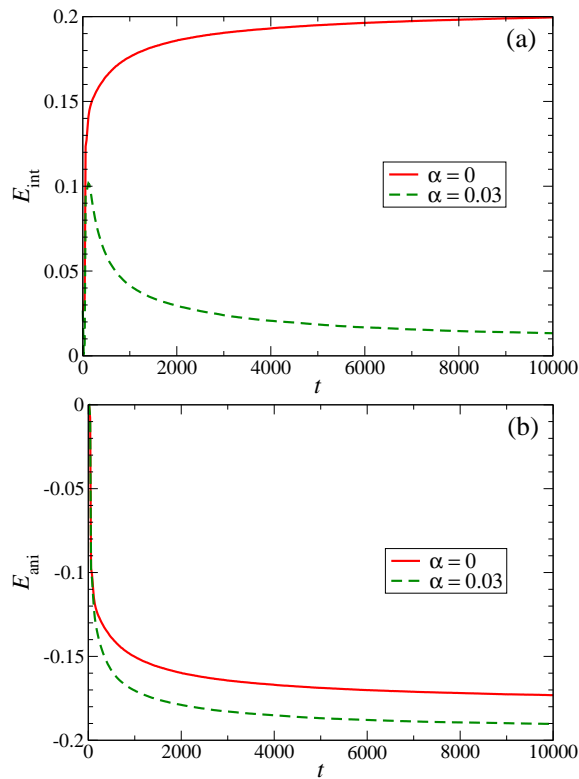


FIG. 2. (Color online) Time dependence of (a) the interfacial energy E_{int} and (b) the anisotropy energy E_{ani} . The interfacial energy increases with time in the no-damping case ($\alpha = 0$) and decreases in the damping case ($\alpha = 0.03$). The anisotropy energy decreases with time in both cases.

as $L(t) \sim t^{1/2}$.

Before discussing growth laws, we should examine scaling laws. The scaled correlation functions of m_z at different times are shown in Fig. 4. At late times, the correlation functions that are rescaled by the average domain size $L(t)$ collapse to a single function. However, the scaled correlation functions at early times ($t = 100$ and 1000) do not agree with the scaling function especially in the short range.

Since scaling behavior is confirmed at late times, the domain growth law is considered to be $L(t) \sim t^{1/2}$ rather than $t^{1/3}$ in this system. In our previous work, we saw domain growth as $L(t) \sim t^{1/3}$ in a BEC without superfluid flow [9], which was essentially the same system as the present one. However, the time region shown in Ref. [9] corresponds to the early stage ($t \lesssim 1830$) in the present system.

Although the growth exponent is supposed to be $n = 1/3$ for conserved scalar fields, the average domain size grows as $L(t) \sim t^{1/2}$, in our system, at late times even in the no-damping case. This implies that our system without damping cannot be categorized as a model of a conserved scalar field. Although we consider m_z as the order parameter to define the characteristic length scale, the LLG equation is described in terms of a vector field

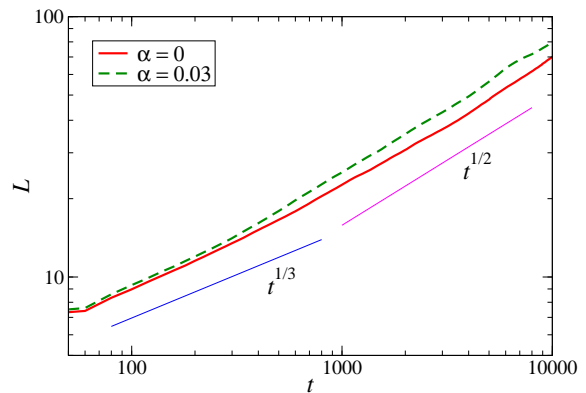


FIG. 3. (Color online) Time dependence of the average domain size L for $\alpha = 0$ and 0.03 . In both damping and no-damping cases, $L(t) \sim t^{1/3}$ at early times and $L(t) \sim t^{1/2}$ at late times.

m_z .

Scaling behavior also appears in the structure factor $S(k, t)$, which is given by the Fourier transformation of the correlation function $G(r)$. According to the Porod law, the structure factor has a power-law tail,

$$S(k, t) \sim \frac{1}{L(t)k^{d+1}}, \quad (7)$$

in high- k regime [1]. Here, d is the dimension of the system. Since $d = 2$ in our system, Eq. (7) leads to $S(k, t)/L(t)^2 \sim [kL(t)]^{-3}$. In Fig. 5, $S(k, t)/L(t)^2$ is plotted as a function of $kL(t)$. The data at different late times collapse to one curve, and they show $S(k) \sim k^{-3}$ in the high- k regime ($kL \sim 10$) in both the damping and no-damping cases. In the ultrahigh- k regime ($kL \sim 100$), tails are different between the two cases, which reflects the difference in domain structure. Since domain walls are fuzzy in the no-damping case, $S(k)$ remains finite. However, in the damping case, $S(k)$ decays faster in the ultrahigh- k regime, which is related with smooth domain walls.

IV. DISCUSSION

We here have a naive question: Why does domain pattern formation occur even in the no-damping case? When $\alpha = 0$, Eq. (2) is just the equation of the precession of spin, and the energy E as well as m_z is conserved. We here discuss why similar domain patterns are formed in both damping and no-damping cases.

Using the stereographic projection of the unit sphere of spin onto a complex plane [14], we rewrite Eq. (4) as

$$\frac{\partial \omega}{\partial t} = \frac{-i + \alpha}{1 + \alpha^2} \left[\nabla^2 \omega - \frac{2\omega^*(\nabla \omega)^2}{1 + \omega\omega^*} - \frac{C_{\text{ani}}\omega(1 - \omega\omega^*)}{1 + \omega\omega^*} \right], \quad (8)$$

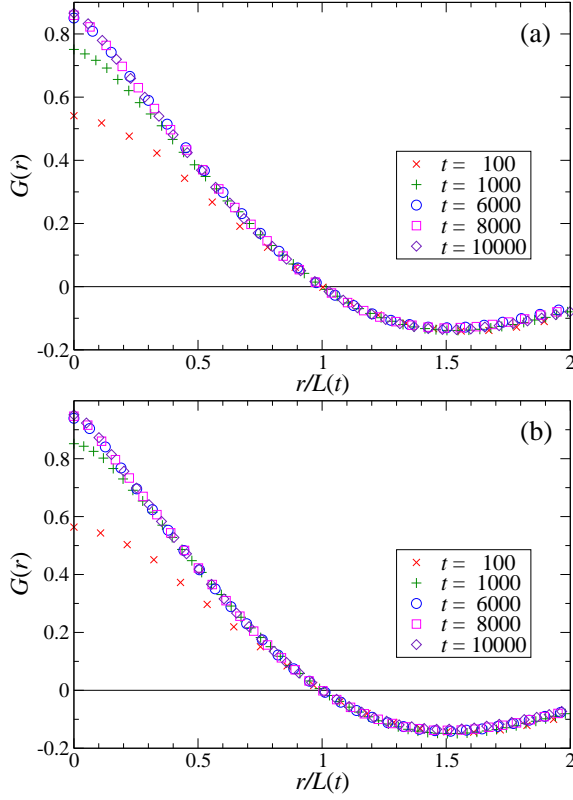


FIG. 4. (Color online) Scaled correlation functions at different times in (a) no-damping ($\alpha = 0$) and (b) damping ($\alpha = 0.03$) cases. The correlation functions at late times collapse to a single function, however, the ones at early times do not.

where ω is a complex variable defined by

$$\omega = \frac{m_x + im_y}{1 + m_z}. \quad (9)$$

Equation (8) implies that the effect of the Gilbert damping is just a rescaling of time by a complex constant [14]. The fixed points of Eq. (8) are $|\omega|^2 = 1$ and $\omega = 0$. The linear stability analysis about these fixed points gives some clues about domain formation.

At the fixed point $\omega = 1$, $m_x = 1$ and $m_y = m_z = 0$, which corresponds to the initial condition of the numerical simulation. Substituting $\omega = 1 + \delta\omega$ into Eq. (8), we obtain linearized equations of $\delta\omega$ and $\delta\omega^*$. Performing Fourier expansions $\delta\omega = \sum_{\mathbf{k}} \delta\tilde{\omega}_{\mathbf{k}} e^{i\mathbf{k}\cdot\mathbf{r}}$ and $\delta\omega^* = \sum_{\mathbf{k}} \delta\tilde{\omega}_{-\mathbf{k}}^* e^{i\mathbf{k}\cdot\mathbf{r}}$, we have

$$\frac{d}{dt} \begin{pmatrix} \delta\tilde{\omega}_{\mathbf{k}} \\ \delta\tilde{\omega}_{-\mathbf{k}}^* \end{pmatrix} = \begin{pmatrix} \tilde{\alpha}_1(C_{\text{ani}} - k^2) & \tilde{\alpha}_1 C_{\text{ani}} \\ \tilde{\alpha}_2 C_{\text{ani}} & \tilde{\alpha}_2(C_{\text{ani}} - k^2) \end{pmatrix} \begin{pmatrix} \delta\tilde{\omega}_{\mathbf{k}} \\ \delta\tilde{\omega}_{-\mathbf{k}}^* \end{pmatrix}, \quad (10)$$

where $\tilde{\alpha}_1 = \frac{1}{2}(-i + \alpha)/(1 + \alpha^2)$, $\tilde{\alpha}_2 = \frac{1}{2}(i + \alpha)/(1 + \alpha^2)$, $\mathbf{k} = (k_x, k_y)$, and $k = |\mathbf{k}|$. The eigenvalues of the 2×2

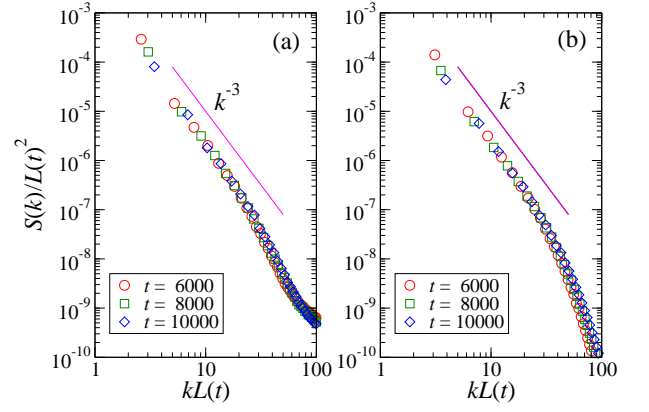


FIG. 5. (Color online) Scaling plots of the structure factor scaled with $L(t)$ at different times in (a) no-damping ($\alpha = 0$) and (b) damping ($\alpha = 0.03$) cases. In both cases, $S(k) \sim k^{-3}$ in the high- k regime. However, they gave different tails in the ultrahigh- k regime.

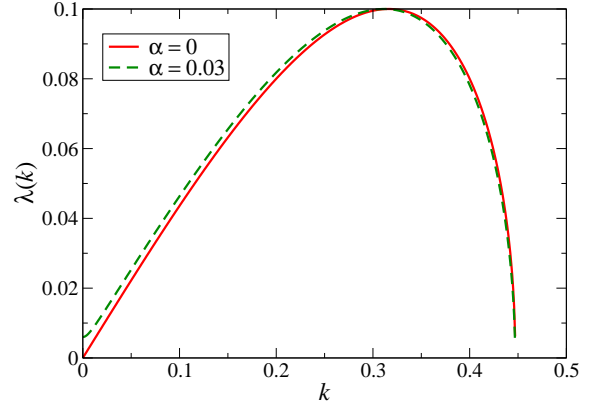


FIG. 6. (Color online) Positive real parts of $\lambda(k)$ that is given by Eq. (11), which has a positive real value for $k < \sqrt{C_{\text{ani}}}$. The difference between $\alpha = 0$ and $\alpha = 0.03$ is small.

matrix of Eq. (10) are

$$\lambda(k) = \frac{\alpha}{2(1 + \alpha^2)}(C_{\text{ani}} - 2k^2) \pm \frac{\sqrt{4k^2(C_{\text{ani}} - k^2) + \alpha^2 C_{\text{ani}}^2}}{2(1 + \alpha^2)}. \quad (11)$$

Even when $\alpha = 0$, $\lambda(k)$ has a positive real part for $k < \sqrt{C_{\text{ani}}}$. Thus, the uniform pattern with $m_x = 1$ is unstable, and inhomogeneous patterns can appear.

The positive real parts of Eq. (11) for $\alpha = 0$ and $\alpha = 0.03$ have close values, as shown in Fig. 6. This corresponds to the fact that domain formation in the early stage has no remarkable difference between the damping ($\alpha = 0.03$) and no-damping ($\alpha = 0$) cases (See Fig. 1). From the view point of energy, the anisotropy energy does not necessarily keep decaying when $\alpha = 0$. For conservation of energy, it should be also possible that both anisotropy and interfacial energies change only a little.

Because of the instability of the initial state, m_z grows, and thus, the anisotropy energy decreases.

The initial condition, which is given as spins aligned in one direction with some noises in the x - y plane, is the key to observe domain pattern formation in the no-damping case. Actually, if spins have totally random directions, no large domains are formed in the no-damping case, although domains are formed in damping cases ($\alpha > 0$) from such an initial state.

When $\omega = 0$, $m_x = m_y = 0$ and $m_z = 1$, which is also one of the fixed points. Substituting $\omega = 0 + \delta\omega$ into Eq. (8) and performing Fourier expansions, we have the linearized equation of $\delta\tilde{\omega}_{\mathbf{k}}$,

$$\frac{d}{dt}\delta\tilde{\omega}_{\mathbf{k}} = \frac{i - \alpha}{1 + \alpha^2}(k^2 + C_{\text{ani}})\delta\tilde{\omega}_{\mathbf{k}}. \quad (12)$$

This implies that the fixed point is stable for $\alpha > 0$ and neutrally stable for $\alpha = 0$. Although $m_z = -1$ corresponds to $\omega \rightarrow \infty$, the same stability is expected for $m_z = -1$ by symmetry.

Since the initial condition is unstable, the z -component of spin grows. Because of the short-range interaction, which is included in the effective field as the Laplacian term of Eq. (3), neighboring spins tend to direct in the same direction. Since $m_z = \pm 1$ are not unstable, m_z can keep its value at around $m_z = \pm 1$. This is why simi-

lar domain patters are formed in both damping and no-damping cases. The difference between the two cases is just that $m_z = \pm 1$ are attracting for $\alpha > 0$ and neutrally stable for $\alpha = 0$.

V. CONCLUSIONS

We have investigated the domain formation in 2D vector fields with an easy-axis anisotropy, using the LLG equation. In both the damping ($\alpha \neq 0$) and no-damping ($\alpha = 0$) cases, the average domain size grows as $L(t) \sim t^{1/3}$ in early times and $L(t) \sim t^{1/2}$ in late times. Since scaling behavior is observed only at late times, the domain growth law in this system is considered as $L(t) \sim t^{1/2}$. The damping gives no remarkable effects on domain growth and large-scale properties of domain pattern. In contrast, small-scale structures are different between the two cases, which is shown quantitatively in the structure factor. This difference is induced by the reduction of the interfacial energy due to the damping.

ACKNOWLEDGMENTS

This work was supported by MEXT KAKENHI (No. 26103514, “Fluctuation & Structure”).

-
- [1] A. Bray, *Adv. Phys.* **43**, 357 (1994)
 - [2] I. M. Lifshitz and V. V. Slyozov, *J. Phys. Chem. Solids* **19**, 35 (1961)
 - [3] C. Wagner, *Z. Elektrochem* **65**, 581 (1961)
 - [4] T. Ohta, D. Jasnow, and K. Kawasaki, *Phys. Rev. Lett.* **49**, 1223 (1982)
 - [5] D. A. Huse, *Phys. Rev. B* **34**, 7845 (1986)
 - [6] A. J. Bray, *Phys. Rev. Lett.* **62**, 2841 (1989)
 - [7] A. J. Bray, *Phys. Rev. B* **41**, 6724 (1990)
 - [8] A. J. Bray and A. D. Rutenberg, *Phys. Rev. E* **49**, R27 (1994)
 - [9] K. Kudo and Y. Kawaguchi, *Phys. Rev. A* **88**, 013630 (2013)
 - [10] J. Hofmann, S. S. Natu, and S. Das Sarma, *Phys. Rev. Lett.* **113**, 095702 (2014)
 - [11] L. A. Williamson and P. B. Blakie, *Phys. Rev. Lett.* **116**, 025301 (2016)
 - [12] H. Furukawa, *Phys. Rev. A* **31**, 1103 (1985)
 - [13] K. Kudo and Y. Kawaguchi, *Phys. Rev. A* **84**, 043607 (2011)
 - [14] M. Lakshmanan and K. Nakamura, *Phys. Rev. Lett.* **53**, 2497 (1984)